The Behavior of a Costas Loop in the Presence of Space Telemetry Signals

T. M. Nguyen
Telecommunications Systems Section

The telemetry modulation index, telemetry bit rate, subcarrier waveform, and subcarrier frequency are shown to be the key system parameters that contribute to the performance degradation of a Costas loop in the presence of space telemetry signals. The effects of the Doppler in the loop are also investigated in this article. The results of this study have been input to the Consultative Committee for Space Data Systems (CCSDS) for consideration in the future standard suppressed-carrier space telemetry system.

I. Introduction

The Consultative Committee for Space Data Systems (CCSDS) has classified space telemetry signals into two categories: Category A, non-deep space missions, and Category B, deep space missions. Category A includes those missions having altitudes above the Earth less than 2×10^6 km, and Category B contains missions having altitudes above the Earth greater than 2×10^6 km. For space telemetry signals, the CCSDS has recommended that a subcarrier be used with a residual carrier when transmitting at low bit rates and that PSK subcarrier modulation be used when a telemetry subcarrier is employed. A square-wave subcarrier is recommended for Category B, and a sine-wave subcarrier for Category A [1].

Costas loop receivers with a residual carrier have been analyzed by M. K. Simon [2]. This analysis has not considered the case where the signal utilizes PSK subcarrier modulation, and also has assumed that the loop phase error approaches zero at a high loop Signal-to-Noise Ratio (SNR) with the Doppler signal being compensated for.

In this article, the performance degradation of the Costas loop in the presence of space telemetry signals is investigated. This represents an extension of [2] to include PSK subcarrier modulation and the presence of Doppler in the input signal. The assumption that the loop phase error approaches zero at a high loop SNR is removed in this analysis. Only the linear approximation which is valid for small phase errors is assumed.

II. Performance of the Costas Loop in the Presence of Deep Space Telemetry Signals

The deep space Category B telemetry signal recommended by the CCSDS can be presented mathematically by [1]

$$S(t) = \sqrt{2P} \cdot \sin(\omega_0 t + m \cdot d(t) \cdot P(t) + \theta(t)) \qquad (1)$$

where P is the total received power, ω_0 is the carrier radian frequency and $\theta(t)$ the corresponding Doppler signal to be estimated, m is the data modulation index with $d(t)$ the NRZ binary valued data sequence, and $P(t)$ is the unit power square-wave subcarrier of frequency f_{sc}.

The above signal is received in the presence of Additive White Gaussian Noise (AWGN), $n(t)$, with

$$n(t) = \sqrt{2}\,[N_c(t)\cos(\omega_0 t + \theta(t)) - N_s(t)\sin(\omega_0 t + \theta(t))]$$

where $N_s(t)$ and $N_c(t)$ are approximately statistically independent, stationary, white Gaussian noise processes with single-sided noise spectral density N_0 W/Hz, and single-sided bandwidth $B_H < (\omega_0/2\pi)$, and the Costas loop is used to track the received signal. If $\phi_e(t)$ denotes the loop phase error, then from previous analysis of this type [2] (assuming $2\phi_e(t)$ is small enough so that the linearizing approximations are applicable, i.e., $\sin(2\phi_e(t)) \approx 2\phi_e(t)$, $\cos(2\phi_e(t)) \approx 1$), we can show that

$$2\phi_e(t) = 2\phi_D(t) + 2\phi_M(t) + 2\phi_N(t) \tag{2}$$

where

$$\phi_D(t) = [1 - H(p)] \cdot \theta(t) \tag{3}$$

$$\phi_M(t) = \frac{P \cdot \sin(2m)}{2\gamma} \cdot H(p) \cdot M_f(t) \tag{4}$$

$$\phi_N(t) = \frac{H(p)}{2\gamma} \cdot N(t, 2\phi_e) \tag{5}$$

Note that the self-noise of data has been assumed to be small so that it can be ignored in the above equations.

Here

$$H(s) = \text{closed-loop transfer function}$$

$$= \frac{\gamma K F(s)}{s + \gamma K F(s)} \tag{6}$$

where

K = (VCO gain) · (phase detector gain)

$F(s)$ = transfer function of loop filter.

$$\gamma = P(\cos^2(m) - \alpha \cdot \sin^2(m)) \tag{7}$$

$$\begin{aligned} N(t, 2\phi_e) = {} & \Big[N_{fs}(t)^2 - N_{fc}(t)^2 + 2\sqrt{P}\,\{N_{fs}(t) \cdot \cos(m) \\ & - M_f(t) \cdot N_{fc}(t) \cdot \sin(m)\}\Big] \cdot (2\phi_e) \\ & + \Big[2 \cdot N_{fs}(t) \cdot N_{fc}(t) + 2\sqrt{P}\,\{N_{fc}(t) \cdot \cos(m) \\ & + M_f(t) \cdot N_{fs}(t) \cdot \sin(m)\}\Big] \end{aligned} \tag{8}$$

Here $M_f(t)$, $N_{fs}(t)$, $N_{fc}(t)$ are the equivalent low-pass arm filtered versions of $M(t)$, $N_s(t)$, $N_c(t)$, respectively. Note that $M(t)$ is the PSK subcarrier modulated data signal which is given by

$$M(t) = d(t) \cdot P(t) \tag{9}$$

As an example, the relationship between $M(t)$ and the filtered version of $M_f(t)$ is given by

$$M_f(t) = G(p) \cdot M(t) \tag{10}$$

where $G(p)$ is the arm filter with p the Heaviside operator.

In Eq. (2) the loop phase error is expressed in terms of the loop phase error due to the Doppler signal ($\phi_D(t)$), loop phase error due to the modulation ($\phi_M(t)$), and phase error due to the noise ($\phi_N(t)$). The factor α in Eq. (7) denotes the modulation distortion factor

$$\alpha = \int_{-\infty}^{\infty} S_M(f)\, |G(j2\pi f)|^2 \cdot df \tag{11}$$

Here $S_M(f)$ denotes the power spectral density of the data modulated subcarrier $M(t)$. It can be shown that for a square-wave subcarrier,

$$S_M(f) = \frac{4}{\pi^2} \sum_{\substack{k=1 \\ k \text{ odd}}}^{\infty} \frac{[S_d(f - kf_{sc}) + S_d(f + kf_{sc})]}{k^2} \tag{12}$$

where $S_d(f)$ is the power spectrum density of the equiprobable NRZ binary telemetry signal.

Let us assume that the initial phase offset of the incoming signal from the phase of the free-running VCO, the data sequence, and the noise are independent. Then, from Eq. (2), the mean-squared tracking phase jitter can be shown to have the form:

$$\sigma^2(\phi_e) = \sigma^2(\phi_D) + \sigma^2(\phi_M) + \sigma^2(\phi_N) \tag{13}$$

where $\sigma^2(\phi_D)$ is the mean-squared tracking phase jitter due to the Doppler signal, $\sigma^2(\phi_M)$ the phase jitter due to modulation produced by the residual carrier, and $\sigma^2(\phi_N)$ the jitter due to the noise. Using [3] it is easy to show that, from Eq. (2),

$$\sigma^2(\phi_D) = \frac{1}{2\pi}\int_{-\infty}^{\infty} |1 - H(j\omega)|^2 \cdot E\{|\theta(j\omega)|^2\} \cdot d\omega \tag{14}$$

$$\sigma^2(\phi_M) = \frac{[P\sin(2m)]^2}{(2\pi)[2\gamma]^2}\int_{-\infty}^{\infty} |H(j\omega)|^2 \cdot S_{Mf}(\omega) \cdot d\omega \tag{15}$$

$$\sigma^2(\phi_N) = \frac{1}{(2\pi)[2\gamma]^2}\int_{-\infty}^{\infty} |H(j\omega)|^2 \cdot S_N(\omega) \cdot d\omega \tag{16}$$

Here,

$E\{|\theta(j\omega)|^2\}$ = spectral density of the Doppler signal $\theta(t)$

$S_{Mf}(\omega)$ = spectral density of the data-modulated subcarrier $M(t)$ after low pass arm filtering $= S_M(\omega) \cdot |G(j2\pi f)|^2$

$S_N(\omega)$ = spectral density of the noise $N(t, 2\phi_e)$.

Since the bandwidths of the process $M_f(t)$ and the noise $N(t, 2\phi_e)$ are very wide with respect to the loop bandwidth B_L, we can approximate Eqs. (15) and (16), respectively, as follows:

$$\sigma^2(\phi_M) \approx \frac{2[P\sin(2m)]^2}{[2\gamma]^2} \cdot B_L \cdot S_{Mf}(0) \tag{17}$$

$$\sigma^2(\phi_N) \approx \frac{2}{[2\gamma]^2} \cdot B_L \cdot S_N(0) \tag{18}$$

Here, we define the loop bandwidth B_L as

$$B_L = \frac{1}{2}\int_{-\infty}^{\infty} |H(j\omega)|^2 \cdot \frac{d\omega}{2\pi} \tag{19}$$

Since the CCSDS has recommended that the subcarrier frequency (f_{sc}) to bit rate (R_s) ratio be an integer [1], the power spectral density $S_{Mf}(\omega)$ of the data-modulated subcarrier $M(t)$ after low pass arm filtering is equal to zero at the origin (see Appendix A). Thus the mean-squared phase jitter due to the modulation is also equal to zero.

If the spectrum of the loop phase error is very narrow compared to the noise component $N_c(t)$ after low pass filtering, so that it is constant relative to the noise components, then we can show that

$$S_N(0) = 2P \cdot N_0\left[4\sigma^2(\phi_e) + 1\right] \times \left[\frac{B'N_0}{P} + |G(0)|^2\cos^2(m) + \beta \cdot \sin^2(m)\right] \tag{20}$$

where

$$B' = \frac{1}{2}\int_{-\infty}^{\infty} |G(j2\pi f)|^4 \cdot df \tag{21}$$

$$\beta = \int_{-\infty}^{\infty} S_M(f)\,|G(j2\pi f)|^4 \cdot df \tag{22}$$

From these results, the mean-squared tracking phase jitter can be shown, after some algebraic manipulations, to be

$$\sigma^2(\phi_e) = \frac{\sigma^2(\phi_D)}{\left[1 - \frac{4}{\rho_L}N(m,\alpha,\beta)\right]} + \frac{N(m,\alpha,\beta)}{\rho_L\left[1 - \frac{4}{\rho_L}N(m,\alpha,\beta)\right]} \tag{23}$$

where $N(m,\alpha,\beta)$ and ρ_L are given by

$$N(m,\alpha,\beta) = \frac{1}{(\cos^2(m) - \alpha \cdot \sin^2(m))} \times \left[\frac{1}{\delta'} + |G(0)|^2\cos^2(m) + \beta \cdot \sin^2(m)\right] \tag{24}$$

$$\rho_L = \text{Loop Signal-to-Noise Ratio (SNR)} = \frac{P}{N_0 B_L} \tag{25}$$

δ' in Eq. (24) is defined as:

$$\delta' = \frac{P}{N_0 B'} \tag{26}$$

Since $\sigma^2(\phi_D)$ and $N(m,\alpha,\beta)$ are always greater than zero, then Eq. (23) makes sense only when $(4/\rho_L) \cdot N(m,\alpha,\beta) < 1$.

Thus, for $(4/\rho_L) \cdot N(m,\alpha,\beta) \ll 1$, Eq. (23) can be approximated as

$$\sigma^2(\phi_e) \approx \sigma^2(\phi_D)\left[1 + \frac{4}{\rho_L} \cdot N(m,\alpha,\beta)\right] + \frac{N(m,\alpha,\beta)}{\rho_L} + \frac{4}{(\rho_L)^2} \cdot N^2(m,\alpha,\beta) \tag{27}$$

The mean-squared tracking phase jitter described in Eq. (27) shows how the Costas loop responds to the deep space telemetry signal. The tracking phase jitter due to the Doppler appears as a high pass function, and the jitter due to noise appears as a low pass function. Since the tracking phase jitter is inversely proportional to $[\cos^2(m) - \alpha \cdot \sin^2(m)]$, the loop will experience a serious degradation in tracking performance when the modulation index m of the data is near m_c (see [2], Eq. (15))

$$m_c = \cot^{-1}(\sqrt{\alpha}) \tag{28}$$

At $m = \cot^{-1}(\sqrt{\alpha})$, the loop will drop lock at any loop SNR.

If the Doppler signal can be compensated for and the loop SNR is very high, then Eq. (28) can be written as:

$$\sigma^2(\phi_e) \approx \frac{N(m,\alpha,\beta)}{\rho_L} \tag{29}$$

If the data does not utilize a square-wave subcarrier, then the result found in Eq. (29) is similar to that found in [2] and [4] (with the ranging channel turned off).

III. Performance of the Costas Loop in the Presence of Non-Deep Space Telemetry

The signal format for non-deep space telemetry is the same as that for deep space except that a sine-wave subcarrier waveform is used in place of the square wave [1]. Letting $M_1(t) = d(t) \cdot \sin(2\pi f_{sc} t)$, and assuming that the arm filters are built such that no spectral components greater than f_{sc} get into the error control signal in the loop, then following the above procedure we can show that the mean-squared tracking phase jitter for this case is (see Appendix B)

$$\sigma'^2(\phi'_e) = \sigma'^2(\phi_D)\left[1 + \frac{4}{\rho_{1L}} \cdot N_1(m', \alpha_1, \beta_1)\right] + \frac{N_1(m', \alpha_1, \beta_1)}{\rho_{1L}} + \frac{4 \cdot N_1^2(m', \alpha_1, \beta_1)}{(\rho_{1L})^2} \tag{30}$$

where $\sigma'^2(\phi'_D)$ is defined as in Eq. (14), with $H(s)$ replaced by $H_1(s)$

$$H_1(s) = \frac{\gamma_1 \cdot K \cdot F(s)}{s + \gamma_1 \cdot K \cdot F(s)}$$

$$\gamma_1 = P[J_0^2(m') - 4 \cdot \alpha_1 \cdot J_1^2(m')] \tag{31}$$

$$N_1(m', \alpha_1, \beta_1) = \frac{[(1/\delta') + 2|G(0)|^2 J_0^2(m') + 4 \cdot \beta_1 \cdot J_1^2(m')]}{[J_0^2(m') - 4 \cdot \alpha_1 \cdot J_1^2(m')]} \tag{32}$$

where α_1 and β_1 are given by

$$\alpha_1 = \int_{-\infty}^{\infty} S_{M1}(f)\,|G(j2\pi f)|^2 \cdot df \tag{33}$$

$$\beta_1 = \int_{-\infty}^{\infty} S_{M1}(f)\,|G(j2\pi f)|^4 \cdot df \tag{34}$$

Here α_1 is the modulation distortion factor, and $S_{M1}(f)$ is the spectral density of $M_1(t)$, which is given by

$$S_{M1}(f) = S_d(f - f_{sc}) + S_d(f + f_{sc}) \tag{35}$$

Note that ρ_{1L} is defined the same as in Eq. (25), with $H_1(s)$ in place of $H(s)$ for the computation of B_L. If the jitter due to Doppler can be compensated for, and the loop SNR is high, then Eq. (30) can be approximated as

$$\sigma'^2(\phi'_e) \approx \frac{N_1(m', \alpha_1, \beta_1)}{\rho_{1L}} \tag{36}$$

The loop will be degraded seriously in tracking performance when the modulation index m' is near the value m'_c, which will satisfy

$$[J_0(m'_c)/J_1(m'_c)]^2 = 4 \cdot \alpha_1 \tag{37}$$

IV. Numerical Examples

It is shown that the Costas loop will be degraded seriously in tracking performance when the modulation index m (or m') is near the critical value, called m_c (or m_c'), which is given by Eqs. (28) and (37) for deep space and non-deep space missions, respectively. The loop will drop lock at any loop SNR when the modulation index satisfies these equations. Therefore, it is crucial to understand the behavior of the modulation distortion factors α and α_1 as a function of data rate, subcarrier frequency, and arm filter noise bandwidth. In this section we will evaluate these distortion factors and illustrate some numerical results for the single-pole Butterworth arm filter.

The transfer function for the single-pole Butterworth filter is given by

$$|G(j2\pi f)|^2 = \frac{1}{1+(f/f_0)^2} \tag{38}$$

where f_0, the 3-dB bandwidth, is related to the two-sided noise bandwidth B_1 of the filter by

$$f_0 = \frac{B_1}{\pi} \tag{39}$$

Substituting Eqs. (38) and (12) into Eq. (11) and rearranging gives the modulation distortion factor α, for Category B, of the form

$$\alpha = \frac{8\cdot (f_0)^2}{\pi^2 T_s} \sum_{\substack{k=1\\ k\ \mathrm{odd}}}^{\infty} \int_{-\infty}^{\infty} \frac{\sin^2(\pi T_s[f-kf_{sc}])}{k^2(f-kf_{sc})^2\,(f^2+f_0^2)} \cdot df \tag{40}$$

where $T_s = (1/R_s)$ is the symbol duration of the telemetry data sequence. In uncoded binary systems, the bit duration equals the symbol duration. Thus, the ratio of subcarrier frequency, f_{sc}, to bit rate, R_s, for this case is

$$f_{sc}\cdot T_s = (f_{sc}/R_s) = n, \qquad n = 1, 2, 3, \ldots \tag{41}$$

Using contour integration and carrying out the necessary mathematics gives

$$\alpha = \frac{4}{\pi^2}\cdot\frac{B_1}{R_s} \sum_{\substack{k=1\\ k\ \mathrm{odd}}}^{\infty} \times \left[a\left(n,k,\frac{B_1}{R_s}\right)\left\{ b\left(n,k,\frac{B_1}{R_s}\right)\left[1-\exp\left(-\frac{2B_1}{R_s}\right)\right] + \frac{2B_1}{R_s}\right\}\right] \tag{42}$$

here $a(\,.\,,\,.\,,\,.\,)$ and $b(\,.\,,\,.\,,\,.\,)$ are given by

$$a(n,k,B_1/R_s) = \frac{1}{k^2\left[(nk\pi)^2 + (B_1/R_s)^2\right]} \tag{43}$$

$$b(n,k,B_1/R_s) = \frac{(nk\pi)^2 - (B_1/R_s)^2}{(nk\pi)^2 + (B_1/R_s)^2} \tag{44}$$

The modulation distortion factor α_1 for Category A telemetry signals can be expressed in terms of $a(\,.\,,\,.\,,\,.\,)$ and $b(\,.\,,\,.\,,\,.\,)$ by evaluating Eq. (33). For this case, it is found that

$$\alpha_1 = \frac{B_1}{R_s}\, a\left(n,1,\frac{B_1}{R_s}\right)\left\{ b\left(n,1,\frac{B_1}{R_s}\right)\left[1-\exp\left(-2\frac{B_1}{R_s}\right)\right] + 2\frac{B_1}{R_s}\right\} \tag{45}$$

The numerical results of Eqs. (42) and (45) are plotted in Figs. 1 and 2, respectively. There, the modulation factors α and α_1 are plotted in decibels versus the ratio (B_1/R_s) for various values of n, the ratio of subcarrier frequency to bit rate. Using these results for α and α_1 in Figs. 1 and 2, the critical modulation index m_c versus the ratio (B_1/R_s) with n as a parameter can be plotted. As an example, Fig. 3 illustrates the critical modulation index m_c for Category B missions as a function of (B_1/R_s). Figures 1 and 2 show that the modulation distortion factors for both Categories A and B decrease as the subcarrier frequency to bit rate ratio, n, increases. The physical meaning for this is that the degradation in tracking performance of the loop is less when we place the data further away from the carrier (at the expense of wider bandwidth). Furthermore, from these figures, we observe that for a given bit rate there exists an optimum noise bandwidth for the arm filters in the sense of minimizing the degradation in mean-squared tracking phase jitter. It is also seen that the degradation in the modulation distortion factor for Category A is more than that of Category B for a given n and (B_1/R_s). Figure 3 shows that the critical modulation index m_c decreases as the noise bandwidth to bit rate ratio (B_1/R_s) increases. Also, m_c is shown to decrease as we place the data closer to the carrier frequency (decreasing in n). This means that the closer we place the data to the carrier, the more power the carrier requires to maintain a proper tracking performance.

V. Conclusions

It has been shown that the Costas loop can be used to track space telemetry signals in the presence of Doppler. This operation can increase mean-squared tracking jitter if there is a residual carrier, as was recommended for both Categories A (non-deep space) and B (deep space) telemetry signals. The performance degradation of the loop can be optimized by choosing a proper subcarrier waveform, subcarrier frequency, bit rate, and arm filter noise bandwidth. This article has numerically evaluated such degradation for single-pole Butterworth arm filters for both Categories A and B. To completely understand the behavior of the Costas loop in the presence of space telemetry signals, the false lock performance still needs to be found.

Acknowledgment

The author is indebted to Dr. M. K. Simon for his valuable comments and helpful suggestions.

References

[1] "Recommendations for Space Data System Standards: Radio Frequency and Modulation Systems, Part 1: Earth Station and Spacecraft," CCSDS 401-B-1, Blue Book, Consultative Committee for Space Data Systems (CCSDS), January 1987.

[2] M. K. Simon, "The Effects of the Residual Carrier on Costas Loop Performance as Applied to the Space Shuttle Orbiter S-Band Uplink," *IEEE Transactions on Communications*, vol. COM-26, no. 11, pp. 1542–1548, November 1978.

[3] A. Papoulis, *Probability, Random Variables, and Stochastic Process*, New York: McGraw-Hill, Chapter 10, 1960.

[4] J. K. Holmes, *Coherent Spread Spectrum Systems*, New York: John Wiley & Sons, Inc., 1982.

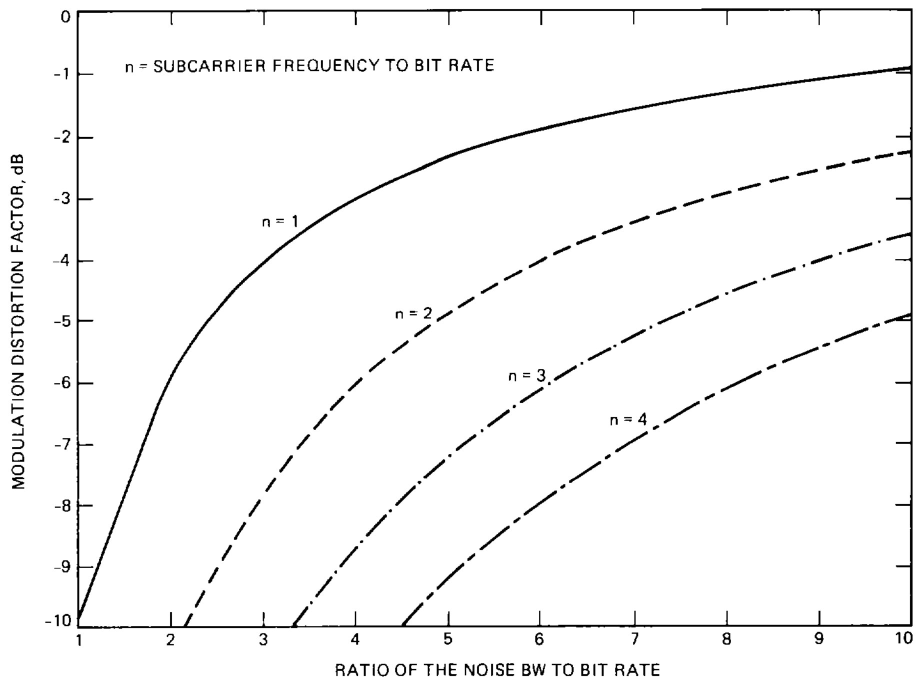

Fig. 1. Modulation distortion factor vs. (B_1/R_s), Category B

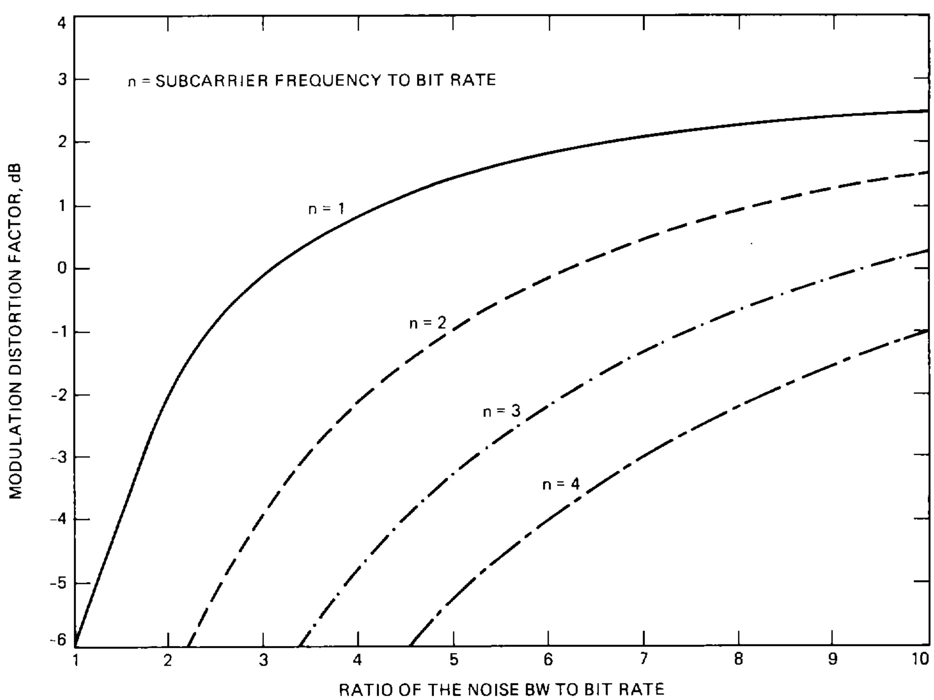

Fig. 2. Modulation distortion factor vs. (B_1/R_s), Category A

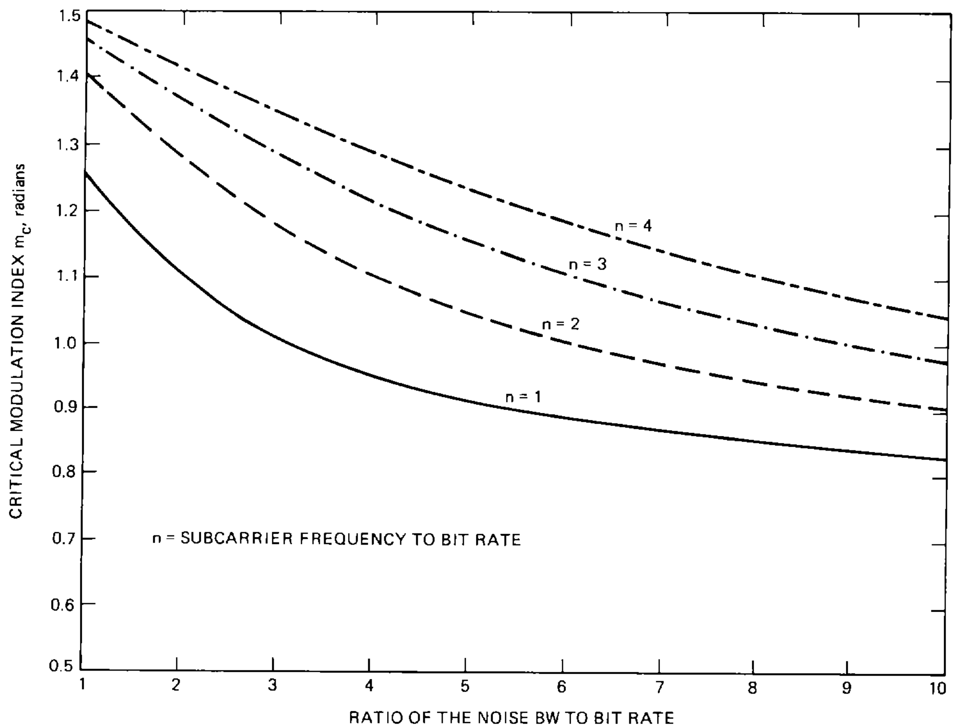

Fig. 3. Critical modulation index m_c vs. (B_1/R_s), Category B

Appendix A

The power spectral density of the data-modulated subcarrier $M(t)$ after low-pass arm filtering is given by

$$S_{Mf}(\omega) = S_M(\omega) \cdot |G(j2\pi f)|^2 \qquad \text{(A-1)}$$

where $S_M(\omega)$ is given in Eq. (12), and $G(\cdot)$ is the transfer function of the low pass arm filter.

Since the CCSDS has recommended that the NRZ binary signal be used for $d(t)$, the power spectrum density $S_d(f)$ of the equiprobable NRZ binary signal is given by

$$S_d(f) = T_s \cdot [\sin(\pi f T_s) / (\pi f T_s)] \qquad \text{(A-2)}$$

The spectral density of the low pass arm filtered data-modulated subcarrier at the origin, for an NRZ binary signal, can be obtained by substituting Eq. (A-2) into Eq. (12), then substituting the result into Eq. (A-1) and evaluating it at $\omega = 2\pi f = 0$. The result is given as follows:

$$S_{Mf}(0) = \frac{8T_s}{\pi^2} \cdot \sum_{\substack{k=1 \\ k \text{ odd}}}^{\infty} \left[\frac{\sin(\pi T_s k f_{sc})}{(\pi T_s k f_{sc})} \right]^2 \cdot \left| \frac{G(0)}{k} \right|^2 \qquad \text{(A-3)}$$

From Eq. (41), the product $(T_s f_{sc})$ always equals an integer. Thus, Eq. (A-3) becomes

$$S_{Mf}(0) = 0 \qquad \text{(A-4)}$$

Appendix B

From Eq. (1), the non-deep space Category A signal can be written as

$$S'(t) = \sqrt{2P}\, J_0(m') \cdot \sin(\omega_0 t + \theta'(t)) + \sqrt{2P}\, J_1(m') \cdot d(t) \cdot \cos(\omega_0 t + \theta'(t)) \tag{B-1}$$

Here we have assumed that

$$20 \log_{10}(J_0(m')) \gg 20 \log_{10}(J_2(m'))$$

$$20 \log_{10}(J_1(m')) \gg 20 \log_{10}(J_3(m'))$$

If the Costas loop is used to track this signal in the presence of AWGN, then the loop phase estimate of $\theta'(t)$, $\hat{\theta}(t)$, can be shown to have the form

$$2\hat{\theta}'(t) = \frac{PKF(s)}{s}\Big[[(J_0(m'))^2 - 4 \cdot \alpha_1 \cdot (J_1(m'))^2]\,(2\phi_e'(t)) + 4J_0(m') \cdot J_1(m') \cdot M_{1f}(t) + n_1(t, 2\phi_e')\Big] \tag{B-2}$$

where

$$\phi_e'(t) = \theta'(t) - \hat{\theta}'(t) = \text{loop phase error} \tag{B-3}$$

$$n_1(t, 2\phi_e') = \Big[N_{fs}(t)^2 - N_{fc}(t)^2 + 2\sqrt{P}\{N_{fs}(t) \cdot J_0(m') - 2M_{1f}(t) \cdot N_{fc}(t) \cdot J_1(m')\}\Big] \cdot (2\phi_e') + \Big[2 \cdot N_{fs}(t) \cdot N_{fc}(t) + 2\sqrt{P}\{N_{fc}(t) \cdot J_0(m') + 2M_{1f}(t) \cdot N_{fs}(t) \cdot J_1(m')\}\Big] \tag{B-4}$$

$$M_{1f}(t) = G(p) \cdot M_1(t),\ M_1(t) = d(t) \cdot \sin(2\pi f_{sc} t) \tag{B-5}$$

It should be noted here that all the other parameters (which are not defined here) have been defined in the preceding sections, and that the previous assumptions (small loop phase error, small self-noise of the modulation) are used in deriving Eq. (B-2).

Let

$$\gamma_1 = P[J_0^2(m') - 4 \cdot \alpha_1 \cdot J_1^2(m')] \tag{B-6}$$

where α_1 is the modulation distortion factor which was defined in Eq. (33).

From Eq. (B-3), Eq. (B-2) can be rearranged as

$$2\phi_e'(t) = 2\phi_D'(t) + 2\phi_M'(t) + 2\phi_N'(t) \tag{B-7}$$

where

$$\phi_D'(t) = [1 - H_1(p)] \cdot \theta'(t) \tag{B-8}$$

$$\phi_M'(t) = \frac{2P \cdot J_0(m') \cdot J_1(M)}{\gamma_1} \cdot H_1(p) \cdot M_{1f}(t) \tag{B-9}$$

$$\phi_N'(t) = \frac{H_1(p)}{2\gamma_1} \cdot n_1(t, 2\phi_e') \tag{B-10}$$

where $H_1(s)$ is the closed-loop transfer function (for this particular case) which is defined in Eq. (31).

Following the procedure in Section II, the mean-squared tracking phase jitter for non-deep space telemetry signals can be shown to take the form expressed in Eq. (30).